Electronic properties of CVD and synthetic diamond

C. E. Nebel, J. Münz, and M. Stutzmann
Walter Schottky Institut, TU-München, Am Coulombwall, D-85748 Garching, Germany

R. Zachai and H. Güttler
Daimler Benz AG, Forschung und Technik, D-89013 Ulm, Germany

(Received 24 September 1996; revised manuscript received 22 November 1996)

Transport and contact properties of synthetic IIb- and intrinsic chemical vapor deposition (CVD) -diamond films are discussed. The samples have been investigated by time-of-flight and transient photoconductivity experiments using Cr/Au contacts. A hole depletion layer at the Cr/Au-IIb-diamond interface and an electron depletion layer at the Cr/Au-CVD-diamond interface is detected. The data indicate that our normally undoped CVD-diamond films are n-type semiconductors. In IIb diamond the mobilities of electrons and holes have been measured, while in CVD diamond no carrier transit can be detected due to the short Schubweg less than or equal to 1 μm. Two trap levels located approximately 190 meV below the conduction band and 670 meV above the valence band are deduced. Electron spin resonance experiments demonstrate that these CVD films are highly defective, containing about 10^{18} cm^{-3} carbon related defects ($g=2.0029$). [S0163-1829(97)00215-4]

I. INTRODUCTION

The structural properties of chemical vapor deposition (CVD) -grown diamond have improved significantly over recent years. Layers with (100) columnar texture are available with thickness ranging up to several hundreds of micrometers.[1] Now the optimization of electronic properties of CVD-diamond films attracts increasing attention in order to realize active or passive electronic devices such as particle detectors, UV sensors, and high-temperature switching devices. The properties of monocrystalline diamond are well known and applications are promising due to the high electron ($2200\,\mathrm{cm}^2/\mathrm{V\,s}$) and hole ($1600\,\mathrm{cm}^2/\mathrm{V\,s}$) mobilities, high saturation carrier velocities (1.5×10^7 cm/s), high electric-field breakdown strength (10^7 V/cm), high intrinsic resistivity (as high as 10^{20} S/cm), and low dielectric constant (5.7).[2] On the other hand, very little is known about the transport properties of synthetic and CVD-diamond films.

In this paper we discuss transport properties measured by time-of-flight and transient photoconductivity experiments, performed in a sandwich contact configuration on synthetic IIb- and CVD-diamond layers. We investigate contact properties of the Cr/Au-diamond interface, bulk properties such as mobilities of electrons and holes in IIb diamond, $\mu\tau$ products, and the Schubweg of carriers in CVD diamond. A brief discussion of the electronic properties with respect to defect densities deduced from electron spin resonance experiments is also given.

II. EXPERIMENT

The CVD-diamond films have been grown by microwave plasma assisted CVD technique, using methane and hydrogen as source gases.[3] No nitrogen has been added intentionally; however, elastic recoil detection experiments reveal residual nitrogen contents of about 10 ppm.[4] The layers were 64 μm thick with (100) texture. Optical micrographs of the surface indicate crystallite sizes of 10–20 μm, while the back side (interface to the Si substrate) shows no texture. The silicon substrate has been removed by a KOH etch. The synthetic IIb-diamond sample has geometric dimensions of $5\times3\times0.5$ mm^3. On the top and back side of each film, semitransparent contacts (25% transmission at 215 nm) with an area of 3 mm^2 have been deposited by subsequent evaporation of Cr/Au. The samples have been illuminated through the top contact.

A time-of-flight setup as shown in Fig. 1 has been used, where a nitrogen pumped dye laser with a frequency-doubling β-barium-borate (BBO) crystal creates laser flashes of 500-ps duration at a wavelength λ_{FD} of 215 nm (5.6 eV). The absorption coefficient of diamond at λ_{FD} measured by

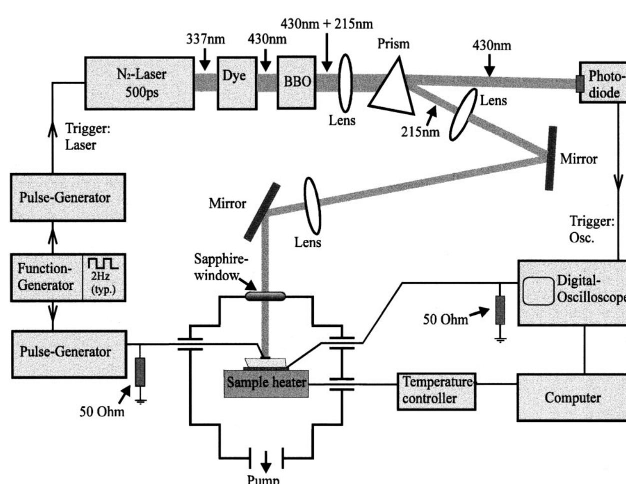

FIG. 1. Time-of-flight setup. A N_2-pumped dye laser with a frequency-doubling BBO crystal is used as the light source. The sample is placed in a cryostat and the field is applied by a pulse generator. Laser emission and pulse generator are triggered by a function generator. The signals are recorded by a fast digital oscilloscope. The setup is controlled by a computer.

0163-1829/97/55(15)/9786(6)/$10.00

© 1997 The American Physical Society

optical transmission experiments is 900 cm^{-1}, indicating that most of the light is absorbed within about 11 μm. For the charge collection and time-of-flight experiments pulsed electric fields F_{ext} of variable strength ($F_{ext} < 2\times10^4$ V/cm) have been applied 1 μs before the laser excitation in order to establish homogeneous fields in the diamond layer between front and back contact. The contact properties were evaluated by transient photoconductivity experiments, which are closely related to the time-of-flight technique. The carriers are generated by a short laser pulse in and close to the depletion layer region. To vary the width of the depletion layer, a dc-bias voltage is applied.

Space-charge limitations of the current transients can be ruled out due to the weak photoexcitation where $Q_{ph} < \frac{1}{10} Q_0$. Here Q_0 is the charge on the electrodes and Q_{ph} is the photogenerated charge of 8×10^{-11} C. The signals have been recorded with a fast digitizing scope (1-GHz resolution) using 50-Ω termination and averaging over 25 transients to improve the signal-to-noise ratio. The samples were placed in a cryostat where the temperature could be varied between 4 and 500 K. To measure the carbon-related ($g=2.0029$) defect density, electron spin resonance (ESR) experiments have been performed on free-standing samples in a standard X-band ESR spectrometer.

III. Cr/Au-DIAMOND CONTACT PROPERTIES

Contact effects arise from space charges that are present at the interface of two materials. The space-charge layer extends over a fraction of the sample thickness, which depends on the type and quality of the material. A Schottky junction in an n-type semiconductor gives rise to an electron depletion layer and in a p-type semiconductor to a hole depletion layer, respectively. A variety of experiments can be applied to study the surface region. It has been shown that transient photoconductivity can be used to explore interface electronic properties.[5] The principle of these experiments is as follows. The light pulse excites a number N_0 of mobile carriers near the one electrode. As the carriers move in the electric field of the depletion layer, there is a charge induced on the opposite electrode of magnitude

$$Q=N_0 e\frac{\bar{x}}{d}, \quad (1)$$

where $\bar{x}$ is the average distance moved by the photogenerated charges and d is the sample thickness. In practice, the photocurrent is the measured quantity and the collected charge Q is obtained by numerical integration. At zero bias the drift of carriers is due to the built-in field in the depletion layer. Application of an external dc field gives rise to an additional field distributed mainly in the contact area of the Schottky barrier. The photocurrent in a nonuniform field is

$$j_{ph}(t)=ne\mu F(t), \quad (2)$$

where $F(t)$ is the field experienced by the charge packet at time t after the excitation pulse, μ is the mobility of carriers, and n is the density of carriers. Provided that both n and μ are independent of time, j_{ph} is directly proportional to $F(t)$. From the sign of the current (charge) one obtains the type of band bending that is a depletion layer either for electrons (n-type material) or for holes (p-type material).

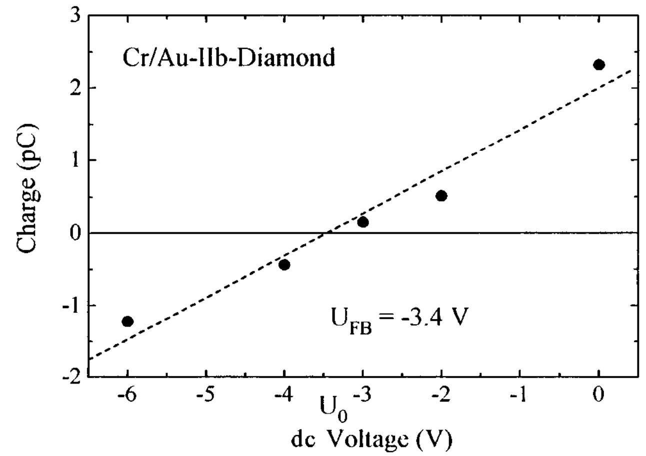

FIG. 2. Charge collection experiments in IIb diamond with Cr/Au contacts. To achieve flat-band conditions ($Q=0$) a dc field of -3.4 V has to be applied (dashed line is for guiding the eye).

Figures 2 and 3 show charge collection data measured at the Cr/Au-IIb-diamond and the Cr/Au-CVD-diamond interface, respectively. In the p-type IIb diamond Q is positive at zero field, indicating a hole depletion layer, while Q is negative in the intrinsic CVD diamond, indicating an electron depletion layer. This result is confirmed by a variety of experiments on different samples containing nitrogen up to 100 ppm and demonstrates that the investigated CVD diamond is an n-type semiconductor. This conclusion is in contradiction to data of Mort, Machonkin, and Okumura, who propose p-type properties of intrinsic CVD diamond based on doping experiments.[6] Given the likely variability in preparation conditions and the high defect densities, this contradiction cannot be resolved based on the presented data. Applying a forward voltage reduces the built-in potential of the illuminated contact. Flat-band conditions, where $Q=0$, are achieved at -3.4 and $+11.3$ V for IIb and CVD diamond, respectively. Due to the presence of Schottky contacts at the front and the back electrode, relatively high voltages have to be applied because most of the dc-bias voltage drops at the reverse biased back contact.

The relaxation of the depletion layer due to an applied external field, which switches the Schottky contact towards

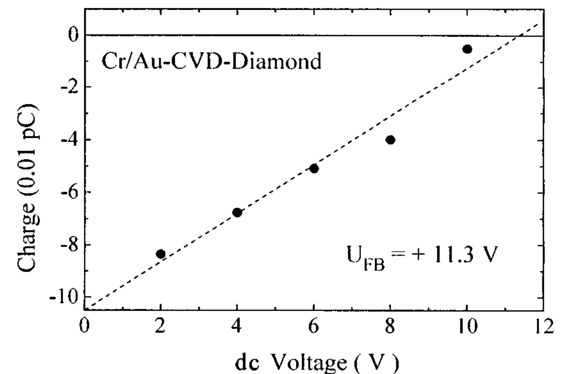

FIG. 3. Charge collection experiments in CVD diamond with Cr/Au contacts. To achieve flat-band conditions ($Q=0$) a dc field of $+11.3$ V has to be applied (dashed line is for guiding the eye).

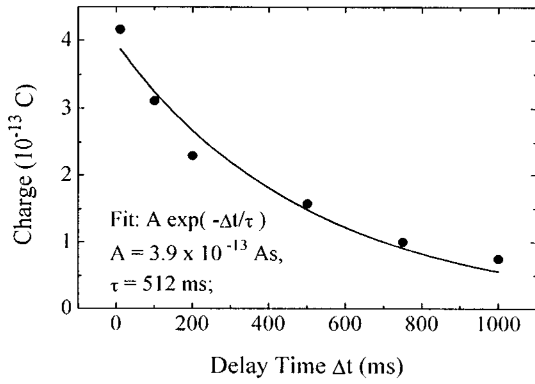

FIG. 4. Depletion layer relaxation in CVD diamond with Cr/Au contacts after application of the flat-band voltage of $+11.3$ V. The full line is the calculated fit to the data.

flat-band conditions, is explored by recording the charge as a function of the delay time between applied field ($t=0$) and the exposure of the contact to a light pulse at time t. Figure 4 shows the result obtained at $T=300$ K on the Cr/Au-CVD-diamond interface, applying $+11.3$ V at $t=0$. The relaxation of the depletion layer towards flat-band conditions proceeds via an exponential time dependence with a time constant τ approximately equal to 500 ms (see the fit in Fig. 4). The energy level of the defect or trap involved can be determined by applying the usual detailed balance arguments

$$\nu(E_T)\tau=1, \tag{3}$$

where $\nu(E_T)$ is the attempt-to-escape frequency of carriers in traps at energy E_T, given by

$$\nu(E_T)=\nu_0 \exp\left(-\frac{E_T}{kT}\right), \tag{4}$$

with ν_0 about 10^{12} s^{-1}. Inserting Eq. (4) into Eq. (3) gives

$$E_T=kT \ln(\nu_0\tau). \tag{5}$$

For $kT=25$ meV and $\tau\cong 500$ ms the trap level E_T is about 670 meV deep in the band gap. The equilibration process is dominated by hole emission, as schematically described in Fig. 5, and the trap level therefore should be about 670 meV above the valence band. This position agrees well with the

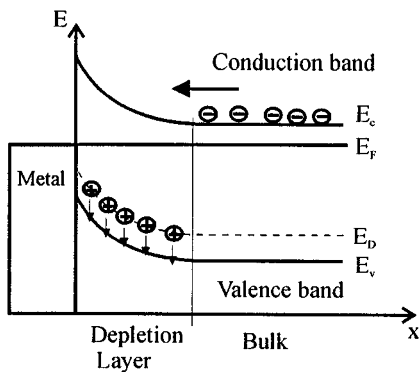

FIG. 5. Schematic view of an electron depletion layer that is switched into the forward direction towards the flat-band case. Before electrons can enter the depletion layer, the holes have to be emitted to vary the depletion layer width.

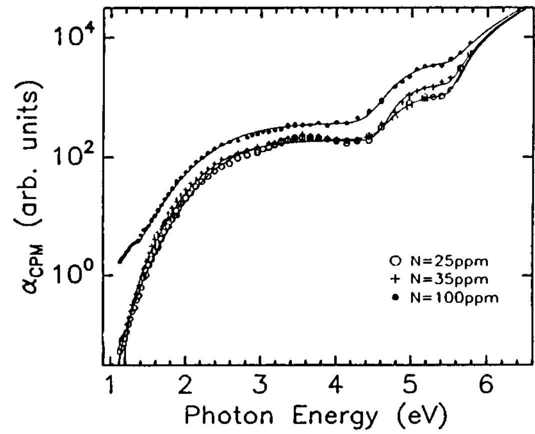

FIG. 6. Absorption coefficient in arbitrary units of CVD diamond with different nitrogen content, measured by constant photocurrent experiments (CPM) from Ref. 10. The defect band at $h\nu>4.8$ eV is identified to rule the depletion layer relaxation experiment.

detected defect distribution measured by constant photocurrent experiments on CVD-diamond films with different nitrogen contents ($10\ \text{ppm}\leq N/C\leq 100\ \text{ppm}$), which is shown in Fig. 6.[7] We assume that optical transitions are from defects into the conduction band, which is expected for an n-type semiconductor, so that $h\nu$ is the energy relative to the conduction band. Taking into account the indirect optical gap E_g of diamond of 5.5 eV and the onset of the broad defect absorption band at about 4.8 eV, we calculate a 0.7-eV gap to the valence band, which is in reasonable agreement with the presented data of 0.67 eV determined by the thermal relaxation experiment. We assume therefore that the depletion relaxation is dominated by hole emission from the defect band detected at $h\nu\geq 4.8$ eV below the conduction band by optical experiments.

IV. BULK ELECTRONIC PROPERTIES

Figure 7 shows typical time-of-flight (TOF) transients measured at 300 K in the IIb-diamond film with Cr/Au contacts. During the laser exposure (500 ps) the photosignal increases towards a maximum and decays after illumination

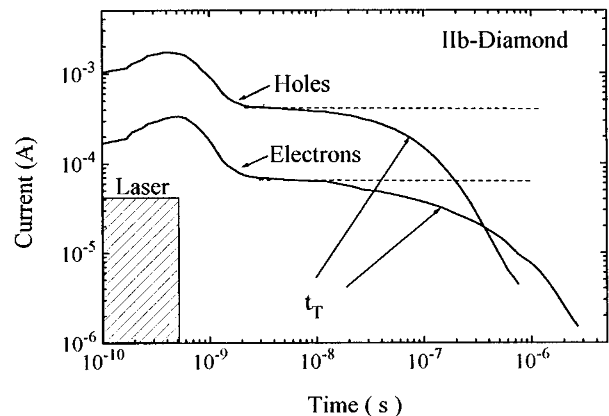

FIG. 7. Electron and hole time-of-flight signals measured in IIb diamond at 300 K and at $F=800$ V/cm. Also shown is the laser excitation duration (shade area).

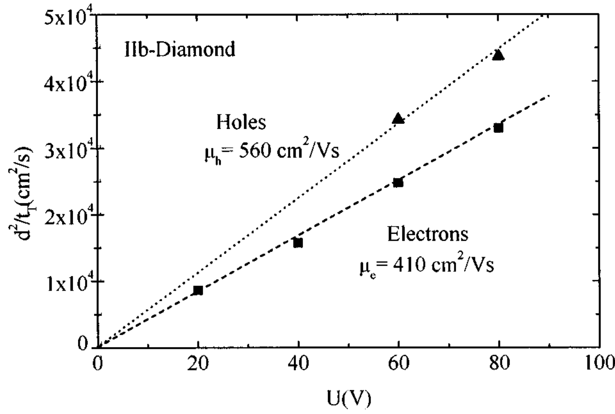

FIG. 8. Transit time t_T versus applied voltage of electrons and holes in IIb diamond at $T = 300$ K ($d = 0.5$ mm). The dashed lines represent a fit of Eq. (6) to the data that gives mobilities of holes and electrons of 560 and 410 cm^2/V s, respectively.

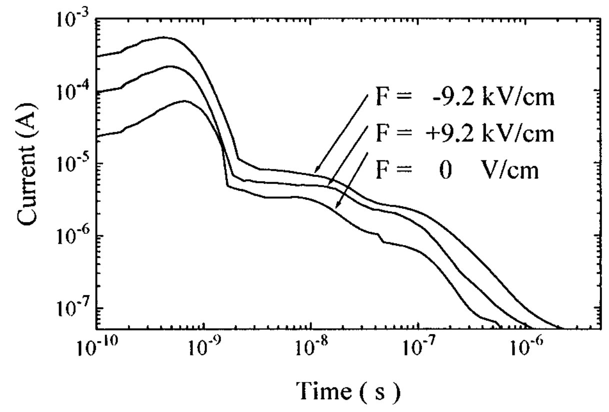

FIG. 10. Transient current decays measured at $T = 300$ K in CVD diamond at different electric fields.

within 2 ns by a factor 4–5. This decay is due to (i) carrier separation because one type of carrier is rapidly extracted via the front contact, dependent on the polarity of the applied field, and (ii) the inhomogeneous electric field in the vicinity of the top contact. The other type of carrier drifts through the bulk of the diamond. For the case $\mu\tau F > d$, where τ is the deep-trapping live time, the current is approximately constant during the charge transit (in Fig. 7 the time regime 2×10^{-9} s$<t<2\times10^{-8}$ s). The arrival of the carriers at the back contact causes a final current decay where the 50% decay relative to the preceding plateau defines the transit time t_T of the center of charge. The mobility can be calculated by

$$\mu = \frac{d^2}{t_T U}, \tag{6}$$

where U is the applied voltage. In Fig. 8 we have plotted d^2/t_T versus U, which increases linearly with increasing applied voltage for both electrons and holes. At $T = 300$ K, the electron mobility is 410 cm^2/V s and the hole mobility is 560 cm^2/V s in IIb diamond, independent of the applied field and in reasonable agreement with the data available in the literature.[8,9]

In the case of $\mu\tau F < d$, carriers are trapped before transit and the $\mu\tau$ product can be evaluated by charge collection measurements where the collected charge $Q(F)$ is obtained by numerical integration of the current

$$Q(F) = \int_0^{t\to\infty} I(t)dt. \tag{7}$$

Charge collection data measured in IIb diamond at $T = 300$ K are shown in Fig. 9. Note that the charge at zero external field is $+1.5\times10^{-11}$ C, which is due to the displacement of carriers in the built-in field of the depletion layer at the Cr/Au-IIb-diamond interface (see above). The $\mu\tau$ product is deduced from a fit of the Hecht equation

$$Q(F)/Q_0 = \frac{\mu\tau F}{d}\left\{1 - \exp\left(-\frac{d}{\mu\tau F}\right)\right\} \tag{8}$$

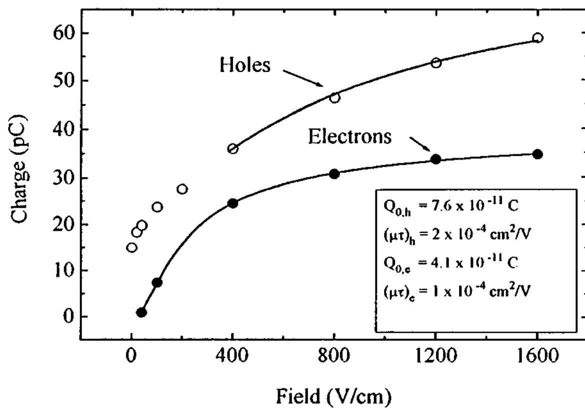

FIG. 9. Charge collection data for electrons and holes in IIb diamond measured at $T = 300$ K. From a fit of the Hecht equation [Eq. (8), full lines] to the data we deduce $\mu\tau$ products of approximately 10^{-4} cm^2/V and a saturation charge collection of (4–7) $\times10^{-11}$ pC for electrons (e) and holes (h).

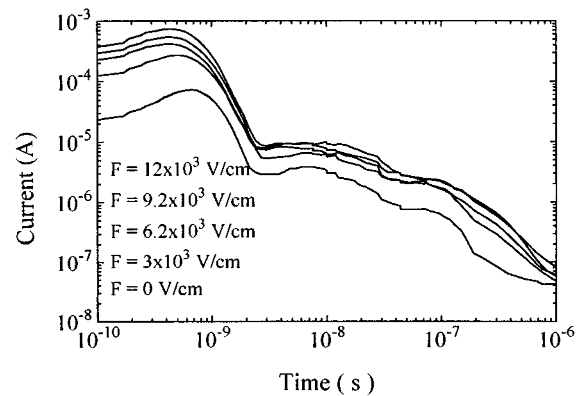

FIG. 11. Field-dependent photocurrents measured in CVD diamond at 300 K.

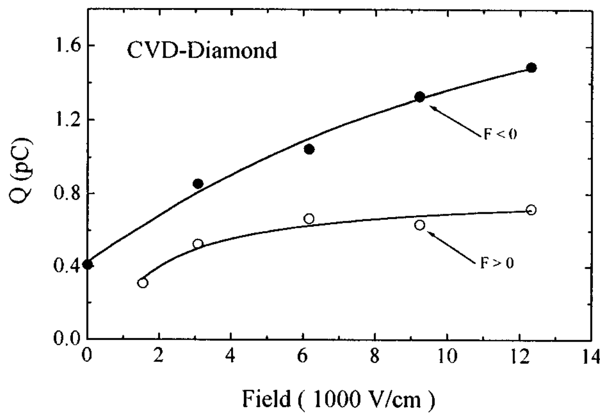

FIG. 12. Charge collection data measured in CVD diamond at $T=300$ K. The charge collected at the highest applied field is 70–100 times smaller than in CVD diamond.

to the data.[10] For both electrons and holes one obtains $(1-2)\times10^{-4}$ cm^2/V. Taking into account the mobilities, the deep trapping lifetime τ of electrons and holes is about $(2-3)\times10^{-7}$ s.

Typical TOF transients measured in an intrinsic CVD-diamond film at $T=300$ K are shown in Fig. 10 (current amplitudes). We detect a similar time dependence as in IIb diamond; however, the field dependence is different. After the maximum at 500 ps the amplitude drops rapidly (2 ns) by a factor 10, passing over to a shoulder with minor substructures and to a final decay for times greater than 10^{-7} s. Reversing the applied electric field results in a reversion of the current, but the characteristics of the time-dependent decay remain nearly unchanged. Even at zero field, the decay is not significantly different. This points toward a trapping and recombination dominated current decay. The field-dependent data shown in Fig. 11 support this argument. The amplitude increases linearly with F, but no transit of carriers can be detected. Carriers are deeply trapped or recombine before transit.

After the initial decay at $t\leqslant10^{-9}$ s a plateau emerges in the time regime 2×10^{-9} s$<t<10^{-8}$ s, indicating a temporary thermal equilibrium between carriers in a shallow trap level and in the conduction band. (We refer to the conduction band because the presented data indicate n-type material where electrons dominate the transport properties.) The energy level in the band gap of diamond can be calculated based on the detailed balance equation given by Eq. (5). Taking into account the time needed to establish a quasiequilibrium less than or equal to 2×10^{-9} s (see Figs. 10 and 11) and assuming $\nu_0\cong10^{12}$ s^{-1} gives $E_c-E_T\leqslant190$ meV. This is a shallow trap level, which up to now has not been detected in diamond by other experiments.

A plot of the charge collection data $Q(F)$, shown in Fig. 12, reveals that $Q(F)$ varies only weakly with increasing electric field. The saturation value Q_s is 6×10^{-13} C for a positive and 1.45×10^{-12} C for a negative electric field. This is about 70–100 times smaller than the charge collected in IIb diamond, $Q_0=7\times10^{-11}$ C. Note that the absorption coefficients at $\lambda=215$ nm of IIb and CVD diamond are comparable. Carriers get deeply trapped or recombine before transit so that the Schubweg w is much smaller than d ($w=\mu\tau F\ll d$). In this case the Hecht equation [Eq. (3)] reduces to

$$Q_s/Q_0=w/d, \tag{9}$$

which results in a Schubweg w of 0.6–1 μm. Taking into account the applied electric field approximately equal to 10^4 V/cm gives $\mu\tau$ products smaller than10^{-8} cm^2/V, which indicates a high defect density. A variety of spectroscopic experiments show that CVD diamond contains predominantly intrinsic or nitrogen-related defects.[7,11] Their interactions with electrons and holes are up to now not very well understood; however, it is reasonable to assume that these centers dominate the electronic properties of CVD diamond. For example, we have measured the carbon-related defect density by electron spin resonance experiments to about 10^{18} cm^{-3} ($g=2.0029$), which can easily explain the small Schubweg detected by charge collection experiments.

V. SUMMARY

The measured electron and hole mobilities in II diamond of 410 and 560 cm^2/V s fit into the broad distribution of data available in the literature, ranging from 500 to 2000 cm^2/V s. The details of this spread have been unclear up to now, but are most likely related to differences in material properties. Due to the difficulties that arise by applying standard Hall experiments on insulating semiconductors such as diamond films, the TOF experiments are an alternative way to investigate transport properties and to correlate the data with impurity densities for example.

Transport in CVD diamond is dominated by fast recombination and trapping of carriers, which limits applications as sensitive photodetectors or particle detectors, where the Schubweg has to be large. The data show that an n-type band bending at the Cr/Au-CVD-diamond interface is present, showing that in our case intrinsic CVD diamond is an n-type semiconductor. Future work must be done to find out if this is a special or general property. The Schubweg w is shorter than 1 μm due to the small $\mu\tau$ products. A shallow trap level located 190 meV below the conduction-band edge and a deep defect/trap 670 meV above the valence band-edge are detected. These results, measured in state-of-the-art CVD-diamond films with relatively little nitrogen incorporated (less than 10 ppm), indicate that further improvements in electronic quality are needed to upgrade CVD diamond for active electronic applications. Especially, the reduction of the defect density towards semiconductor standards will be especially a challenge for the near future.

ACKNOWLEDGMENT

The project has been supported by the Bundesministerium für Bildung und Forschung of Germany under Contract No. 3N1001G4.

[1] G. Davies, *Properties and Growth of Diamond* (Inspec, London, 1994).

[2] M. Buckley-Golder and A. T. Collins, Diamond Relat. Mater. **1**, 1083 (1992).

[3] H. J. Füßer, M. Rösler, M. Hartweg, R. Zachai, X. Jiang, and C. P. Klages, Proceedings of the Third International Symposium on Diamond Materials [Electrochem. Soc. **93-17**, 102 (1993)].

[4] A. Bergmaier, G. Dollinger, T. Faestermann, C. M. Frey, M. Ferguson, H. Güttler, G. Schultz, and H. Willerscheid, in Proceedings of Diamond Films, Barcelona, 1995 [Diamond Relat. Mater. (to be published)].

[5] R. A. Street, Phys. Rev. B **27**, 4924 (1983).

[6] J. Mort, M. A. Machonkin, and K. Okumura, Appl. Phys. Lett. **59**, 455 (1991).

[7] E. Rohrer, C. F. O. Graeff, R. Janssen, C. E. Nebel, M. Stutzmann, H. Güttler, and R. Zachai, Phys. Rev. B **54**, 7874 (1996).

[8] P. R. de la Houssaye, C. M. Penchina, C. A. Hewett, G. R. Wilson, and J. M. Zeidler, J. Appl. Phys. **71**, 3220 (1992).

[9] J. A. von Windheim, V. Venkatesan, D. M. Malta, and K. Das, Diamond Relat. Mater. **2**, 841 (1993).

[10] K. Hecht, Z. Phys. **77**, 235 (1932).

[11] C. F. O. Graeff, E. Rohrer, C. E. Nebel, M. Stutzmann, H. Güttler, and R. Zachai (unpublished).